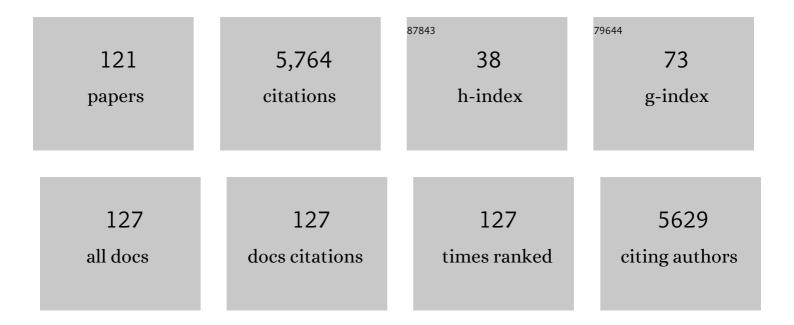
List of Publications by Year in descending order

Source: https://exaly.com/author-pdf/7936763/publications.pdf Version: 2024-02-01



#	Article	IF	CITATIONS
1	Efficacy and safety of selective internal radiotherapy with yttrium-90 resin microspheres compared with sorafenib in locally advanced and inoperable hepatocellular carcinoma (SARAH): an open-label randomised controlled phase 3 trial. Lancet Oncology, The, 2017, 18, 1624-1636.	5.1	595
2	[18F]fluoro-2-deoxy-D-glucose positron emission tomography (FDG-PET) in aggressive lymphoma: an early prognostic tool for predicting patient outcome. Blood, 2005, 106, 1376-1381.	0.6	482
3	Early 18F-FDG PET for Prediction of Prognosis in Patients with Diffuse Large B-Cell Lymphoma: SUV-Based Assessment Versus Visual Analysis. Journal of Nuclear Medicine, 2007, 48, 1626-1632.	2.8	357
4	Personalised versus standard dosimetry approach of selective internal radiation therapy in patients with locally advanced hepatocellular carcinoma (DOSISPHERE-01): a randomised, multicentre, open-label phase 2 trial. The Lancet Gastroenterology and Hepatology, 2021, 6, 17-29.	3.7	307
5	An international confirmatory study of the prognostic value of early PET/CT in diffuse large B-cell lymphoma: comparison between Deauville criteria and ΔSUVmax. European Journal of Nuclear Medicine and Molecular Imaging, 2013, 40, 1312-1320.	3.3	235
6	Prognostic Value of Interim 18F-FDG PET in Patients with Diffuse Large B-Cell Lymphoma: SUV-Based Assessment at 4 Cycles of Chemotherapy. Journal of Nuclear Medicine, 2009, 50, 527-533.	2.8	229
7	Pretherapy metabolic tumour volume is an independent predictor of outcome in patients with diffuse large B-cell lymphoma. European Journal of Nuclear Medicine and Molecular Imaging, 2014, 41, 2017-2022.	3.3	187
8	Interim [¹⁸ F]Fluorodeoxyglucose Positron Emission Tomography Scan in Diffuse Large B-Cell Lymphoma Treated With Anthracycline-Based Chemotherapy Plus Rituximab. Journal of Clinical Oncology, 2012, 30, 184-190.	0.8	152
9	Metabolic tumour volumes measured at staging in lymphoma: methodological evaluation on phantom experiments and patients. European Journal of Nuclear Medicine and Molecular Imaging, 2014, 41, 1113-1122.	3.3	152
10	Whole-body diffusion-weighted magnetic resonance imaging with apparent diffusion coefficient mapping for staging patients with diffuse large B-cell lymphoma. European Radiology, 2010, 20, 2027-2038.	2.3	145
11	Automatic lesion detection and segmentation of 18F-FET PET in gliomas: A full 3D U-Net convolutional neural network study. PLoS ONE, 2018, 13, e0195798.	1.1	112
12	Total metabolic tumor volume, circulating tumor cells, cell-free DNA: distinct prognostic value in follicular lymphoma. Blood Advances, 2018, 2, 807-816.	2.5	107
13	Usefulness of ^{99m} Tc-HMDP scintigraphy for the etiologic diagnosis and prognosis of cardiac amyloidosis. Amyloid: the International Journal of Experimental and Clinical Investigation: the Official Journal of the International Society of Amyloidosis, 2015, 22, 210-220.	1.4	91
14	Improvement of Early ¹⁸ F-FDG PET Interpretation in Diffuse Large B-Cell Lymphoma: Importance of the Reference Background. Journal of Nuclear Medicine, 2010, 51, 1857-1862.	2.8	86
15	Good clinical practice recommendations for the use of PET/CT in oncology. European Journal of Nuclear Medicine and Molecular Imaging, 2020, 47, 28-50.	3.3	85
16	Metastatic Renal Cell Carcinoma: Relationship Between Initial Metastasis Hypoxia, Change After 1 Month's Sunitinib, and Therapeutic Response: An ¹⁸ F-Fluoromisonidazole PET/CT Study. Journal of Nuclear Medicine, 2011, 52, 1048-1055.	2.8	82
17	Optimization of Aerosol Deposition by Pressure Support in Children with Cystic Fibrosis. American Journal of Respiratory and Critical Care Medicine, 2000, 162, 2265-2271.	2.5	79
18	Lymph node imaging: Basic principles. European Journal of Radiology, 2006, 58, 338-344.	1.2	77

#	Article	IF	CITATIONS
19	Whole-Body Diffusion-Weighted Imaging With Apparent Diffusion Coefficient Mapping for Treatment Response Assessment in Patients With Diffuse Large B-Cell Lymphoma. Investigative Radiology, 2011, 46, 341-349.	3.5	73
20	Fully automatic segmentation of diffuse large B cell lymphoma lesions on 3D FDG-PET/CT for total metabolic tumour volume prediction using a convolutional neural network European Journal of Nuclear Medicine and Molecular Imaging, 2021, 48, 1362-1370.	3.3	70
21	FDG PET/CT imaging as a biomarker in lymphoma. European Journal of Nuclear Medicine and Molecular Imaging, 2015, 42, 623-633.	3.3	68
22	Sentinel node localization should be interpreted with caution in midline vulvar cancer. Gynecologic Oncology, 2005, 97, 151-154.	0.6	64
23	Bone marrow involvement in diffuse large B-cell lymphoma: correlation between FDG-PET uptake and type of cellular infiltrate. European Journal of Nuclear Medicine and Molecular Imaging, 2009, 36, 745-750.	3.3	63
24	Validation of a Standardized Normalization Template for Statistical Parametric Mapping Analysis of 123I-FP-CIT Images. Journal of Nuclear Medicine, 2007, 48, 1459-1467.	2.8	57
25	Phase II study of sirolimus in treatment-naive patients with advanced hepatocellular carcinoma. Digestive and Liver Disease, 2012, 44, 610-616.	0.4	57
26	Baseline Total Metabolic Tumor Volume Measured with Fixed or Different Adaptive Thresholding Methods Equally Predicts Outcome in Peripheral T Cell Lymphoma. Journal of Nuclear Medicine, 2017, 58, 276-281.	2.8	55
27	Development and Application of a Real-Time On-Line Blinded Independent Central Review of Interim Pet Scans to Determine Treatment Allocation in Lymphoma Trials. Journal of Clinical Oncology, 2009, 27, 2739-2741.	0.8	54
28	[18F]-NaF PET/CT imaging in cardiac amyloidosis. Journal of Nuclear Cardiology, 2016, 23, 846-849.	1.4	54
29	Long-term follow-up of cognitive dysfunction in patients with aluminum hydroxide-induced macrophagic myofasciitis (MMF). Journal of Inorganic Biochemistry, 2011, 105, 1457-1463.	1.5	50
30	Whole-Body Diffusion-weighted Imaging in Hodgkin Lymphoma and Diffuse Large B-Cell Lymphoma. Radiographics, 2015, 35, 747-764.	1.4	50
31	Changes in cerebral metabolism are detected prior to perfusion changes in early HIV-CMC: A coregistered1H MRS and SPECT study. Journal of Magnetic Resonance Imaging, 2000, 12, 859-865.	1.9	48
32	Obinutuzumab vs rituximab for advanced DLBCL: a PET-guided and randomized phase 3 study by LYSA. Blood, 2021, 137, 2307-2320.	0.6	48
33	An 18F-FDG-PET maximum standardized uptake value > 10 represents a novel valid marker for discerning Richter's Syndrome. Leukemia and Lymphoma, 2016, 57, 1474-1477.	0.6	47
34	Positron emission tomography/computed tomography with 18F-fluorocholine improve tumor staging and treatment allocation in patients with hepatocellular carcinoma. Journal of Hepatology, 2018, 69, 336-344.	1.8	47
35	Interim18F-fluorodeoxyglucose positron emission tomography in diffuse large B-cell lymphoma: qualitative or quantitative interpretation – where do we stand?. Leukemia and Lymphoma, 2009, 50, 1753-1756.	0.6	46
36	The predictive value of treatment response using FDG PET performed on day 21 of chemoradiotherapy in patients with oesophageal squamous cell carcinoma. A prospective, multicentre study (RTEP3). European Journal of Nuclear Medicine and Molecular Imaging, 2013, 40, 1345-1355.	3.3	41

#	Article	IF	CITATIONS
37	Use of Model-Based Iterative Reconstruction (MBIR) in reduced-dose CT for routine follow-up of patients with malignant lymphoma: dose savings, image quality and phantom study. European Radiology, 2015, 25, 2362-2370.	2.3	37
38	18F-FDG PET/CT predicts microvascular invasion and early recurrence after liver resection for hepatocellular carcinoma. Hpb, 2019, 21, 739-747.	0.1	37
39	Whole-body diffusion magnetic resonance imaging in the assessment of lymphoma. Cancer Imaging, 2012, 12, 403-408.	1.2	35
40	Early Phase 99Tc-HMDP Scintigraphy for the Diagnosis and Typing of Cardiac Amyloidosis. JACC: Cardiovascular Imaging, 2017, 10, 601-603.	2.3	33
41	Early-phase myocardial uptake intensity of 99mTc-HMDP vs 99mTc-DPD in patients with hereditary transthyretin-related cardiac amyloidosis. Journal of Nuclear Cardiology, 2018, 25, 217-222.	1.4	30
42	Natural history and impact of treatment with tafamidis on major cardiovascular outcomeâ€free survival time in a cohort of patients with transthyretin amyloidosis. European Journal of Heart Failure, 2021, 23, 264-274.	2.9	30
43	Clinical impact of contrast-enhanced computed tomography combined with low-dose ¹⁸ F-fluorodeoxyglucose positron emission tomography/computed tomography on routine lymphoma patient management. Leukemia and Lymphoma, 2014, 55, 2887-2892.	0.6	29
44	Prognostic value of anthropometric measures extracted from whole-body CT using deep learning in patients with non-small-cell lung cancer. European Radiology, 2020, 30, 3528-3537.	2.3	27
45	MRI and PET in monitoring response in lymphoma. Cancer Imaging, 2005, 5, S106-S112.	1.2	26
46	Distribution of ventilation/perfusion ratios in pulmonary embolism: an adjunct to the interpretation of ventilation/perfusion lung scans. Journal of Nuclear Medicine, 2002, 43, 1596-602.	2.8	26
47	Early Interim PET Scans in Diffuse Large B-Cell Lymphoma: Can There Be Consensus About Standardized Reporting, and Can PET Scans Guide Therapy Choices?. Current Hematologic Malignancy Reports, 2012, 7, 193-199.	1.2	25
48	Respective prognostic values of germinal center phenotype and early 18fluorodeoxyglucose-positron emission tomography scanning in previously untreated patients with diffuse large B-cell lymphoma. Haematologica, 2007, 92, 778-783.	1.7	24
49	Metabolic Tumour Burden Measured by 18F-FDG PET/CT Predicts Malignant Transformation in Patients with Neurofibromatosis Type-1. PLoS ONE, 2016, 11, e0151809.	1.1	23
50	Apical sparing pattern of left ventricular myocardial 99mTc-HMDP uptake in patients with transthyretin cardiac amyloidosis. Journal of Nuclear Cardiology, 2018, 25, 2072-2079.	1.4	23
51	18F-sodium fluoride PET/MRI myocardial imaging in patients with suspected cardiac amyloidosis. Journal of Nuclear Cardiology, 2021, 28, 1586-1595.	1.4	23
52	Dopamine transporter imaging under high-dose transdermal nicotine therapy in Parkinson's disease: an observational study. Nuclear Medicine Communications, 2009, 30, 513-518.	0.5	22
53	Breast Radiotherapy (RT) Using Tangential Fields (TgF): A Prospective Evaluation of the Dose Distribution in the Sentinel Lymph Node (SLN) Area as Determined Intraoperatively by Clip Placement. Annals of Surgical Oncology, 2014, 21, 3758-3765.	0.7	22
54	Whole-Body Functional MRI and PET/MRI in Multiple Myeloma. Cancers, 2020, 12, 3155.	1.7	22

#	Article	IF	CITATIONS
55	Assessment of ejection fraction with Tl-201 gated SPECT in myocardial infarction: Precision in a rest-redistribution study and accuracy versus planar angiography. Journal of Nuclear Cardiology, 2001, 8, 31-39.	1.4	21
56	Functional imaging of hepatocellular carcinoma using diffusion-weighted MRI and 18F-FDG PET/CT in patients on waiting-list for liver transplantation. Cancer Imaging, 2016, 16, 4.	1.2	21
57	Whole body MRI and PET/CT in haematological malignancies. Cancer Imaging, 2007, 7, S88-S93.	1.2	20
58	Patients with Plasma Cell Disorders Examined at Whole-Body Dynamic Contrast-enhanced MR Imaging: Initial Experience. Radiology, 2009, 250, 905-915.	3.6	19
59	Neuropsychological Correlates of Brain Perfusion SPECT in Patients with Macrophagic Myofasciitis. PLoS ONE, 2015, 10, e0128353.	1.1	18
60	Extracardiac soft tissue uptake, evidenced on early 99mTc-HMDP SPECT/CT, helps typing cardiac amyloidosis and demonstrates high prognostic value. European Journal of Nuclear Medicine and Molecular Imaging, 2020, 47, 2396-2406.	3.3	18
61	Hepatobiliary MR contrast agent uptake as a predictive biomarker of aggressive features on pathology and reduced recurrence-free survival in resectable hepatocellular carcinoma: comparison with dual-tracer 18F-FDG and 18F-FCH PET/CT. European Radiology, 2020, 30, 5348-5357.	2.3	17
62	Rituximab plus gemcitabine and oxaliplatin (R-GemOx) in refractory/relapsed diffuse large B-cell lymphoma: a real-life study in patients ineligible for autologous stem-cell transplantation. Leukemia and Lymphoma, 2021, 62, 2161-2168.	0.6	17
63	[F-18]-Fluoro-2-deoxy-d-glucose positron emission tomography as a tool for early detection of immunotherapy response in a murine B cell lymphoma model. Cancer Immunology, Immunotherapy, 2007, 56, 1163-1171.	2.0	15
64	Quantitative lung perfusion scan as a predictor of aerosol distribution heterogeneity and disease severity in children with cystic fibrosis. Nuclear Medicine Communications, 2004, 25, 563-569.	0.5	14
65	Low Suvmax Measured on Baseline FDG-PET/CT and Elevated β2 Microglobulin Are Negative Predictors of Outcome in High Tumor Burden Follicular Lymphoma Treated By Immunochemotherapy: A Pooled Analysis of Three Prospective Studies. Blood, 2016, 128, 1101-1101.	0.6	14
66	Quantitative CT analysis for assessing response in lymphoma. Cancer Imaging, 2005, 5, S102-S106.	1.2	13
67	Brain ¹⁸ F-FDG PET Metabolic Abnormalities in Patients with Long-Lasting Macrophagic Myofascitis. Journal of Nuclear Medicine, 2017, 58, 492-498.	2.8	13
68	History of extracardiac/cardiac events in cardiac amyloidosis: prevalence and time from initial onset to diagnosis. ESC Heart Failure, 2021, 8, 5501-5512.	1.4	11
69	Assessing Cardiac Amyloidosis SubtypesÂby Unsupervised Phenotype Clustering Analysis. Journal of the American College of Cardiology, 2021, 78, 2177-2192.	1.2	11
70	Assessment of myocardial reperfusion after myocardial infarction using automatic 3-dimensional quantification and template matching. Journal of Nuclear Medicine, 2004, 45, 1981-8.	2.8	11
71	Can the Interim Fluorodeoxyglucose–Positron Emission Tomography Standardized Uptake Value Be Used to Determine the Need for Residual Mass Biopsy After Dose-Dense Immunochemotherapy for Advanced Diffuse Large B-Cell Lymphoma?. Journal of Clinical Oncology, 2010, 28, e719-e720.	0.8	10
72	Cognitive dysfunction associated with aluminum hydroxide-induced macrophagic myofasciitis: A reappraisal of neuropsychological profile. Journal of Inorganic Biochemistry, 2018, 181, 132-138.	1.5	10

#	Article	IF	CITATIONS
73	Health-related quality of life in locally advanced hepatocellular carcinoma treated by either radioembolisation or sorafenib (SARAH trial). European Journal of Cancer, 2021, 154, 46-56.	1.3	10
74	Diagnostic Value of 99mTc-HMDP Bone Scan in Atypical Osseous Tuberculosis Mimicking Multiple Secondary Metastases. Spine, 2004, 29, E85-E87.	1.0	9
75	Clinical routine use of dopamine transporter imaging in 516 consecutive patients. Journal of Neurology, 2015, 262, 909-915.	1.8	9
76	Early 18fluorodeoxyglucose PET Scan as a Prognostic Tool in Diffuse Large B-Cell Lymphoma Patients Treated with An Anthracycline-Based Chemotherapy Plus Rituximab Blood, 2009, 114, 98-98.	0.6	9
77	Subacute dopaâ€responsive parkinsonism after successful surgical treatment of aqueductal stenosis. Movement Disorders, 2009, 24, 2438-2440.	2.2	8
78	Characterization of 18-Fluorodeoxyglucose Uptake Pattern inÂInfective Endocarditis After Transcatheter Aortic Valve Implantation. JACC: Cardiovascular Imaging, 2019, 12, 930-932.	2.3	8
79	Clinical impact of dual-tracer FDOPA and FDG PET/CT for the evaluation of patients with parkinsonian syndromes. Medicine (United States), 2020, 99, e23060.	0.4	8
80	Optimization of whole-body 2-[18F]FDG-PET/MRI imaging protocol for the initial staging of patients with myeloma. European Radiology, 2021, , 1.	2.3	8
81	Macrophagic myofasciitis-associated dysfunctioning: An update of neuropsychological and neuroimaging features. Best Practice and Research in Clinical Rheumatology, 2018, 32, 640-650.	1.4	7
82	FDG-PET/CT Brain Findings in a Patient With Macrophagic Myofasciitis. Nuclear Medicine and Molecular Imaging, 2016, 50, 80-84.	0.6	6
83	Baseline Metabolic Tumor Volume Is Predictive of Patient Outcome in Diffuse Large B Cell Lymphoma. Blood, 2012, 120, 1598-1598.	0.6	6
84	Cerebral 18F-FDG PET in macrophagic myofasciitis: An individual SVM-based approach. PLoS ONE, 2017, 12, e0181152.	1.1	6
85	Brain 18F-FDG PET Metabolic Abnormalities in Macrophagic Myofasciitis: Are They Stable?. Journal of Nuclear Medicine, 2017, 58, 1532.2-1533.	2.8	5
86	Renal Infarction and Its Consequences for Renal Function in Patients With Cardiac Amyloidosis. Mayo Clinic Proceedings, 2019, 94, 961-975.	1.4	5
87	Impact of the 18F-FDG-PET/MRI on Metastatic Staging in Patients with Hepatocellular Carcinoma: Initial Results from 104 Patients. Journal of Clinical Medicine, 2021, 10, 4017.	1.0	5
88	Prolonged Remissions After Nivolumab Plus Gemcitabine/Oxaliplatin in Relapsed/Refractory T-cell Lymphoma. HemaSphere, 2022, 6, e672.	1.2	5
89	99mTc-HMDP scintigraphy rectifies wrong diagnosis of AL amyloidosis. Journal of Nuclear Cardiology, 2015, 22, 853-857.	1.4	4
90	Predictive value of brain 18F-FDG PET/CT in macrophagic myofasciitis?. Medicine (United States), 2017, 96, e8134.	0.4	4

#	Article	IF	CITATIONS
91	A rare presentation of skull-base osteomyelitis with neurovascular sheath extension following external otitis resolved by PET/MRI. European Journal of Nuclear Medicine and Molecular Imaging, 2018, 45, 2025-2025.	3.3	4
92	Effectiveness and Safety of Subcutaneous Rituximab for Patients With Gastric MALT Lymphoma: A Case–Control Comparison With Intravenous Rituximab. Clinical Lymphoma, Myeloma and Leukemia, 2021, 21, e32-e38.	0.2	4
93	Cost-Utility Analysis of Transarterial Radioembolization With Yttrium-90 Resin Microspheres Compared With Sorafenib in Locally Advanced and Inoperable Hepatocellular Carcinoma. Clinical Therapeutics, 2021, 43, 1201-1212.	1.1	4
94	Utility of Early Posttreatment PET/CT Evaluation Using FDG or 18F-FCH to Predict Response to 90Y Radioembolization in Patients With Hepatocellular Carcinoma. American Journal of Roentgenology, 2021, , .	1.0	4
95	Postinfectious encephalitis: a coregistered SPECT and magnetic resonance imaging study. Clinical Nuclear Medicine, 2002, 27, 129-130.	0.7	4
96	Echocardiographic Patterns of Left Ventricular Diastolic Function in Cardiac Amyloidosis: An Updated Evaluation. Journal of Clinical Medicine, 2021, 10, 4888.	1.0	4
97	Whole-Body Diffusion-weighted MR Imaging of Iron Deposits in Hodgkin, Follicular, and Diffuse Large B-Cell Lymphoma. Radiology, 2018, 286, 560-567.	3.6	3
98	18F-FDG Whole-body PET/MRI of a 30-Week Pregnant Woman With Breast Cancer Revealed Interesting Fetal Findings. Clinical Nuclear Medicine, 2019, 44, 818-820.	0.7	3
99	FDG PET/CT of Cervical Gout With Spinal Cord Compression. Clinical Nuclear Medicine, 2020, 45, e29-e31.	0.7	3
100	Early Response Evaluation with 18FDG-PET Scanning, but Not Phenotypic Profile, Are Predictive of Outcome in Diffuse Large B-Cell Lymphoma Blood, 2005, 106, 1914-1914.	0.6	3
101	Scintimammography for the Diagnosis of Breast Cancer. Journal of Women's Imaging, 2002, 4, 66-72.	0.2	2
102	Brain 18F-FDG, 18F-Florbetaben PET/CT, 123I-FP-CIT SPECT and Cardiac 123I-MIBG Imaging for Diagnosis of a "Cerebral Type" of Lewy Body Disease. Nuclear Medicine and Molecular Imaging, 2016, 50, 258-260.	0.6	2
103	Dropped head syndrome with proximal myopathy revealing AL amyloidosis. Joint Bone Spine, 2018, 85, 779-781.	0.8	2
104	Prognostic Value of Baseline Quantitative PET Metrics for Patients with Unfavourable Early Stage Hodgkin Lymphoma Enrolled in the Standard Arm of the EORTC/Lysa/FIL H10 Trial. Blood, 2016, 128, 184-184.	0.6	2
105	Rituximab Plus Gemcitabine and Oxaliplatin (R-GemOx) in Refractory/Relapsed (R/R) DLBCL. a Real Life Study in Patients Ineligible for Autologous Transplantation. Blood, 2019, 134, 4115-4115.	0.6	2
106	[18F]Fluorodeoxyglucose Triple-Head Coincident Imaging as an Adjunct to 1311 Scanning for Follow-Up of Papillary Thyroid Carcinoma. Endocrine Practice, 2003, 9, 273-279.	1.1	1
107	Meningeal Metastasis Relapse With Focal Involvement of Cranial Bone Flap. Clinical Nuclear Medicine, 2019, 44, e315-e317.	0.7	1
108	Rituximab or rituximab plus chlorambucil for translocation (11;18)-negative gastric mucosa-associated lymphoid tissue lymphoma: a monocentric non-randomized observational study. Leukemia and Lymphoma, 2022, 63, 2597-2603.	0.6	1

#	Article	IF	CITATIONS
109	"THE UNVEILED HEART―a teaching program in cardiovascular nuclear medicine. Nuclear Instruments and Methods in Physics Research, Section A: Accelerators, Spectrometers, Detectors and Associated Equipment, 2004, 527, 130-133.	0.7	0
110	Functional Imaging in Lymphoma. , 2014, , 1311-1334.		0
111	Amylose AL révélée par un syndrome de la tête tombante avec myopathie proximale. Revue Du Rhumatisme (Edition Francaise), 2019, 86, 529-531.	0.0	0
112	Recommandations et référentiels. Medecine Nucleaire, 2019, 43, 1-4.	0.2	0
113	Shunt Imaging in a Complex Congenital Cardiomyopathy. Clinical Nuclear Medicine, 2000, 25, 827-828.	0.7	0
114	Response Assessment after an Inductive CHOP or CHOP-Like Regimen with or without Rituximab in 103 Patients with Diffuse Large B-Cell Lymphoma (DLBCL): Integrating 18Fluorodeoxyglucose Positron Emission Tomography (PET) to the International Workshop Criteria (IWC) Blood, 2006, 108, 2735-2735.	0.6	0
115	Prognostic Value of Early 18fluorodeoxyglucose PET Scan in Patients with Diffuse Large B Cell Lymphoma Treated with Rituximab Plus CHOP or High-Dose CHOP Blood, 2008, 112, 2006-2006.	0.6	0
116	Number of Circulating t(14;18) Tumor Cells at Diagnosis Is Related to, but Add to the Prognostic Value of Metabolic Tumor Burden in Follicular Lymphoma. Blood, 2015, 126, 3872-3872.	0.6	0
117	Breast Implant Associated-Anaplastic Large Cell Lymphoma (BIA-ALCL): The French Lymphoma Study Association (LYSA) Registry Data. Blood, 2018, 132, 1641-1641.	0.6	0
118	Breast Implant Associated-Anaplastic Large Cell Lymphoma (BIA-ALCL): The Lymphoma Study Association (LYSA) Registry Data. Blood, 2019, 134, 4021-4021.	0.6	0
119	A Molecular Classifier Increased the Accuracy of Lymphoma Diagnosis By Expert Pathologists in the Diffuse Large B-Cell Lymphoma Gained Trial from the Lysa. Blood, 2021, 138, 3495-3495.	0.6	0
120	Breast Implant Associated-Anaplastic Large-Cell Lymphoma (BIA-ALCL): Data Based on the Lymphoma Study Association (LYSA) Registry. Promising Results of Brentuximab Vedotin Combined with Cyclophosphamide, Doxorubicin and Prednisone (BV-CHP) As First Line Treatment for Patient Requiring Chemotherapy. Blood, 2021, 138, 1387-1387.	0.6	0
121	Integrative Study of a High-Grade B-Cell Lymphoma Cohort of 45 Patients: A Single Institution Real Life Study. Blood, 2021, 138, 4576-4576.	0.6	0